American Mineralogist, Volume 90, pages 1648–1654, 2005

# Optic properties of centimeter-sized crystals determined in air with the spindle stage using EXCALIBRW

MICKEY E. GUNTER,[1,*] ROBERT T. DOWNS,[2] KURT L. BARTELMEHS,[3] STANLEY H. EVANS,[4] CAROLYN J.S. POMMIER,[5] JACK S. GROW,[1] MATTHEW S. SANCHEZ,[1] AND F. DONALD BLOSS[6]

[1]Department of Geological Sciences, University of Idaho, Moscow, Idaho 83844, U.S.A.
[2]Department of Geological Sciences, University of Arizona, Tucson, Arizona 85721, U.S.A.
[3]Aces It Group, University of Texas, Austin, Texas 78712, U.S.A.
[4]3701 North Allwood Place, Tucson, Arizona 85750, U.S.A.
[5]Bristol-Myers Squibb, P.O. Box 191, New Brunswick, New Jersey 08903, U.S.A.
[6]Department of Geological Sciences, Virginia Tech, Blacksburg, Virginia 24061, U.S.A.

## ABSTRACT

Extinction data sets for four centimeter-sized anisotropic crystals were collected in air with standard spindle-stage methods and submitted to a new Windows-based version of EXCALIBR, termed EXCALIBRW. EXCALIBRW solved these data sets with varying degrees of accuracy related to the external shape of the crystal: the more rounded the crystal, the more precise the results. For an olivine crystal ground into a sphere, the results were similar to those obtained for a crystal immersed in an index-matching fluid. However, even for samples bounded with growth or cleavage faces, the program determined the orientation of the optical indicatrix and 2V with an error of only 1–2°. Thus, this logical extension of spindle-stage methods is helpful: (1) to orient centimeter-size single crystals for various types of mineralogical measurements (e.g., spectroscopy or diffusion studies in which it might be undesirable to place the sample in a liquid); (2) as a non-destructive means of identifying gemstones based upon a determination of their optical class (i.e., isotropic vs. uniaxial vs. biaxial); and (3) for optical characterization by determination of 2V. In addition, the newest version of EXCALIBR is easier to use, mathematically more robust in its solution algorithms, and provides solutions for crystals in less favorable orientations than the earlier versions of EXCALIBR.

## INTRODUCTION

The spindle stage has been in use since the early 1900s (Gunter 2004; Gunter et al. 2004; and reference therein) as a means to orient single crystals on a polarizing light microscope, but it was not until the work of Wilcox (1959) in the late 1950s, followed by Bloss and coworkers in the late 20$^{th}$ century, that the spindle stage became a robust mineralogical research tool. [See the preface of Bloss (1999), Gunter (2004), and Gunter et al. (2004), for some historical perspectives and Bloss (1981, 1999) and Gunter et al. (2004) for a thorough discussion on the use of the spindle stage in research and teaching.] The major contributions made by Bloss and coworkers over the past 30 years were the refinement of spindle-stage hardware and the development of the computer program EXCALIBR (Bloss and Riess 1973), which solved extinction data sets (i.e., microscope stage settings that cause a crystal to go extinct as the spindle stage is incremented, see Table 1) to yield the orientation of the biaxial indicatrix and determined a precise value of 2V.

The 1973 version of EXCALIBR was improved upon and thoroughly discussed in Bloss (1981), further refined and made PC/Mac compatible in 1988 (Gunter et al. 1988), then completely rewritten and renamed EXCALIBR II in 1992 (Bartelmehs et al. 1992). EXCALIBR II has been improved further and the DOS interface has been replaced with a Windows Graphical User Interface (Gunter et al. 2004 and discussed herein). The major goal of the present paper is to introduce EXCALIBRW to the mineralogical community and show its use with centimeter-sized single crystals whose extinction data sets are collected in air rather than the normal data collection on micrometer-sized crystals whose extinction data sets are routinely collected in index-matching fluids. (The most recent version of EXCALIBRW can be obtained for free by contacting Stanley Evans at Stanley_Evans@comcast.net.)

## EXPERIMENTAL METHODS

### EXCALIBRW

This newest version of EXCALIBR was tested on large samples whose extinction positions had been measured in air and one smaller sample that was measured in an index-matching fluid for comparison (i.e., treated as a control). The newest version of EXCALIBR is a revised version of EXCALIBR II (Bartelmehs et al. 1992), which in turn was a completely rewritten version of EXCALIBR (Bloss 1981; Gunter et al. 1988). EXCALIBR II introduced several improvements over EXCALIBR, mainly: (1) the extinction positions could be measured at any *S* value (i.e., spindle-stage setting) and were not restricted to 10° increments; (2) the input data were free format; and (3) several bugs were fixed, notably the standard error calculations for 2V, for the orientation of optical directions, and for the statistical algorithm used to determine whether dispersion of a given optical direction occurred when extinction data sets were collected at multiple wavelengths. EXCALIBRW further improves on EXCALIBRII in that the program is Windows compatible and creates a user interface that is self-explanatory (Fig. 1). Moreover, EXCALIBRW

* E-mail mgunter@uidaho.edu

0003-004X/05/0010–1648$05.00/DOI: 10.2138/am.2005.1892 

**Table 1.** Input data and results for an ~200 μm olivine crystal measured in the normal manner in an index-matching fluid

san carlos from xanes
Experimental Treatment ID number = 999.0
Refined Reference Azimuth, *M*r = 181.52
Biaxial Results
Counterclockwise Stage
Number of iterations(100 max.) = 11
*R*-squared = 0.99854

| *S* | *M*s | *E*s | CALC(*E*s) | *E*s-CALC(*E*s) |
|---|---|---|---|---|
| 0.00 | 39.90 | 38.38 | 38.42 | –0.04 |
| 10.00 | 36.60 | 35.08 | 35.06 | 0.02 |
| 20.00 | 32.30 | 30.78 | 31.35 | –0.58 |
| 30.00 | 29.90 | 28.38 | 27.66 | 0.72 |
| 40.00 | 25.60 | 24.08 | 24.18 | –0.10 |
| 50.00 | 22.40 | 20.88 | 21.01 | –0.13 |
| 60.00 | 19.60 | 18.08 | 18.08 | 0.00 |
| 70.00 | 16.80 | 15.28 | 15.24 | 0.04 |
| 80.00 | 14.00 | 12.48 | 12.20 | 0.28 |
| 90.00 | 9.60 | 8.08 | 8.44 | –0.36 |
| 100.00 | 4.20 | 2.68 | 3.00 | –0.32 |
| 110.00 | 356.20 | 174.68 | 174.21 | 0.46 |
| 120.00 | 343.00 | 161.48 | 161.22 | 0.26 |
| 130.00 | 330.30 | 148.78 | 148.57 | 0.21 |
| 140.00 | 322.10 | 140.58 | 141.04 | –0.46 |
| 150.00 | 319.10 | 137.58 | 137.91 | –0.33 |
| 160.00 | 319.00 | 137.48 | 137.54 | –0.06 |
| 170.00 | 320.80 | 139.28 | 138.96 | 0.32 |
| 180.00 | 323.00 | 141.48 | 141.58 | –0.10 |

Optic Axial Angle, 2V (ese) = 91.715 (0.636)

Computed Cartesian Coordinates

| | x (ese) | y (ese) | z (ese) |
|---|---|---|---|
| OA1 | –0.7672 (0.0041) | –0.1076 (0.0063) | 0.6323 (0.0050) |
| OA2 | 0.3170 (0.0049) | 0.8199 (0.0034) | 0.4767 (0.0053) |
| AB | –0.7554 (0.0019) | –0.6462 (0.0020) | 0.1084 (0.0031) |
| OB | –0.3232 (0.0036) | 0.5114 (0.0056) | 0.7962 (0.0048) |
| ON | 0.5700 (0.0038) | –0.5664 (0.0044) | 0.5952 (0.0063) |

Spindle Stage Coordinates to measure refractive indices.

| | *S* (ese) | *E*s (ese) | *M*s | |
|---|---|---|---|---|
| OA1 | 99.66 (0.57) | 140.10 (0.36) | | |
| OA2 | 30.18 (0.36) | 71.52 (0.30) | (e-w polr.) | (n-s polr.) |
| AB | 170.48 (0.26) | 139.06 (0.17) | 320.58 | 230.58 |
| OB | 57.29 (0.44) | 108.86 (0.22) | 290.38 | 200.38 |
| ON | 133.58 (0.50) | 55.25 (0.27) | 236.77 | 146.77 |

*Notes:* Graphical results are shown in Figure 2. Five columns are shown in the upper portion of the table labeled: *S* (the spindle-stage setting), *M*s (the microscope stage setting that caused extinction at *S*), *E*s (which is *E* angle and relates to *M*s), CALC(*E*s) (the calculated *E*s values based on the EXCALIBRW solution to the extinction data set), *E*s-CALC(*E*s) (the difference between the observed and calculated *E*s values, these values give an indication of how well the observed and calculated extinction data sets match). Next is listed the calculated value of 2V and its estimated standard error. The next two sections of the table give the orientations of the five optical directions: OA1 and OA2 are the two optic axes and AB, OB, and ON are the acute bisectrix, obtuse bisectrix, and optic normal. In the upper table, the orientations are given in Cartesian coordinates (with associated estimated standard errors), whereas in the lower table, the orientations are cast into the *S* and *E*s spindle stage / microscope stage system. The last two columns of the lower table give the *M*s (i.e., microscope stage settings) to orient AB, OB, or ON in the plane of the stage of the microscope and parallel to the lower polarizer to measure their refractive index.

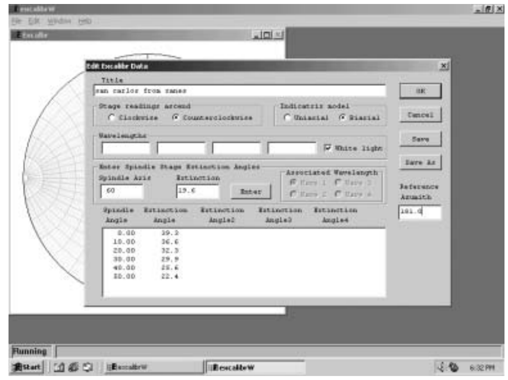

**Figure 1.** Screen capture of the input data window for EXCALIBRW. The input areas and the radio buttons are explained in the text. After all of the data have been input, clicking on the "OK" button will solve the data set, producing a numerical output (e.g., Tables 1–5) and a graphical output (Figs. 2, 4, 5, 8, and 10).

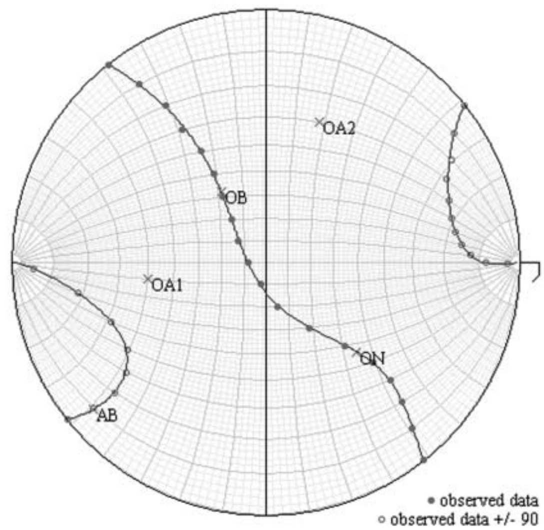


**Figure 2.** Graphical output produced by EXCALIBRW for an olivine grain whose extinction data were collected in a refractive-index-matching fluid. The stereographic projection shows the observed extinction positions (as solid and hollow dots), the calculated extinction curves, the location of the five optical directions, which include the two optic axes (OA1 and OA2) and three mutually perpendicular directions AB, OB, and ON, which are the acute bisectrix, obtuse bisectrix, and optic normal, and geometrically define the biaxial indicatrix. (The graphical output in this figure corresponds to the numerical input in Table 1.)

uses a mathematically more robust algorithm to yield solutions even for crystals in less favorable orientations (i.e., those in which a principal vibration direction is nearly parallel to the spindle axis or where an optic axis is nearly perpendicular to the spindle axis), although some orientations may still fail, and a routine was added that refines the reference azimuth (*M*r) value (where *M*r is the microscope stage setting that orients the spindle stage E-W with the spindle's rotation drum to the user's right).

## Sample selection

Five samples were selected to test EXCALIBRW, and extinction measurements were made on: (1) a ~200 μm San Carlos olivine single crystal; (2) a partially rounded, ~6 mm San Carlos single crystal; (3) an angular fragment of quartz, ~10 mm long, showing crystal faces; (4) an ~10 mm spodumene crystal bounded by cleavage faces; and (5) a sphere of olivine ($Fo_{92}$) ~4 mm in diameter. The extinction data for all five samples (except the 200 μm olivine) were collected in air. The extinction data for the 200 μm olivine sample were collected in an index-matching fluid and served as a control for the accuracy and precision of 2V for the larger San Carlos olivine (in air) and to compare the precision of the orientation. The different morphologies (angular to rounded to sphere) were selected on the assumption that the more spherical the sample, the easier it would be to obtain precise extinction positions, and in turn for EXCALIBRW to provide better 2V and orientational results with lower errors. This holds true because refraction will occur whenever a light ray travels between materials of differing refractive index at non-normal incidence. Thus, for the case of a sphere, normal incidence can be guaranteed, whereas for angular crystals, some refraction will occur, and in extreme cases, total reflection may occur and extinction positions may not be observable. This is the main reason for immersing crystals in an index-matching fluid (i.e., to minimize refraction at the grain boundary interface).

### Optical directions vs. crystallographic directions

By definition, the optical orientation of a mineral relates the mineral's principal vibration directions (E and O for uniaxial minerals and X, Y, and Z for biaxial minerals) to the mineral's crystallographic axes (**a, b, c**). The principal refractive index directions are found by some optical method (e.g., use of the spindle stage and the polarized light microscope), whereas the crystallographic directions are found indirectly by morphology and/or cleavage or directly by a diffraction method (e.g., determination of the orientation matrix with the aid of a single crystal X-ray diffractometer). For the uniaxial case, (i.e., minerals belonging to the tetragonal and hexagonal crystal systems), the E direction always corresponds to the ***c*** crystallographic axis, whereas the biaxial case (i.e., minerals belonging to the orthorhombic, monoclinic, and triclinic crystal systems) is more complex. The biaxial indicatrix is composed of a set of three mutually perpendicular vibration directions (X, Y, Z) that coincide with the three principal refractive index directions ($n_\alpha$, $n_\beta$, $n_\gamma$). Thus for orthorhombic minerals where the three crystallographic directions (**a**, **b**, **c**) are also mutually perpendicular, the optical and crystallographic direction coincide with each other in one of six possible permutations. For the monoclinic case, one of the three optical directions must coincide with the **b** crystallographic axis; however the other two directions are in the same plane as the **a** and **c** crystallographic axes (which are, in general, at a non-90° angle to each other) and do not, except by chance, coincide with any crystallographic axes. Finally, for the triclinic case, where the crystallographic axes are, in general, inclined to each other at non-90° angles, the optical directions do not coincide with any of the crystallographic directions, except by chance; the optical orientation would be given by noting the angular relationships between these two separate vectors sets. The methods described herein will locate the optical directions. To determine how the crystallographic directions relate to these optical directions, one must either perform a diffraction experiment (see Gunter and Twamley 2001) on the same sample or look up the optical orientation in a mineralogical reference text. [The above paragraph is a very brief overview of the optical orientation of minerals. For a thorough discussion, see Bloss (1981). For a method to determine the optical orientation of minerals, see Gunter and Twamley (2001) and for an example of the usefulness of knowing the optical orientation of minerals in spectroscopic studies, see Dyar et al. (2002a, 2002b)].

## Using Excalibrw

Figure 1 shows the input window for EXCALIBRW and should be self-explanatory, especially for those accustomed to using earlier versions of EXCALIBR. The user must stipulate whether the calibrations for the microscope stage ascend in a clockwise or counterclockwise direction. Also, one should employ the biaxial model unless the crystal is known to be uniaxial. Either white light or monochromatic illumination can be chosen next. If extinction data are collected for more than one monochromatic wavelength, the program will perform a dispersion analysis (Gunter et al. 2004). Next, one simply enters the extinction position (*M*s) for different settings of the spindle stage (*S*). The program automatically increments *S* by 10° and, typically, one would like to collect an extinction data set from *S* = 0 to 180° in 10° increments, although this is not necessary for a solution by EXCALIBRW. It is also essential to estimate the reference azimuth (*M*r), which is the microscope stage setting that orients the spindle stage rotation axis E-W with the spindle dial to the user's right (see Bloss 1981 or 1999 for methodology). After an extinction data set has been entered, it is advisable to click the "save as" button and save using a file name of your choice. Finally, when "OK" is selected, EXCALIBRW will attempt to solve the extinction data set. It might fail if the crystal is in a non-favorable orientation, such as a principal vibration direction being near parallel or an optic axis being near perpendicular to the spindle-stage axis. In earlier use of EXCALIBR, special methods were employed to check or to refine the orientation of the grain to determine if a solution would be found (i.e., the 40° test); however, with the improved version of EXCALIBRW, it is more efficient to mount a crystal and collect extinction data than to spend the time trying to refine the grain's orientation. (See Gunter et al. 2004 for a thorough discussion of the advantages and disadvantages of refining grain orientations prior to data collection).

## Results and discussion

### Olivine in oil and air

Figure 2 and Table 1 show the graphical and numerical results for the 200 μm olivine single crystal immersed in an index-matching fluid. One of the major advantages of EXCALIBRW is the graphical output that shows the observed extinction data (solid and open dots), the calculated extinction curves, and the five optical directions. Notice how well the observed and calculated data are in agreement. The numerical results (Table 1) are presented in a similar fashion to earlier versions of EXCALIBR. (See the caption in Table 1 to explain the output fully.) The extinction data set for the small olivine grain was collected with a Leitz Ortholux polarizing microscope in normal configuration.

By comparison, the same microscope is shown in Figure 3, in which the substage condenser system and all the optical components above the stage were removed; thus no optical elements remain on the scope. Next, sheets of polarizing filters were placed below the stage and above the sample. Also note the large, rounded olivine crystal mounted on the end of the goniometer head with beeswax. In this configuration, an extinction data set was collected for this 6 mm San Carlos olivine sample and submitted to EXCALIBRW for solution. Figure 4 is the graphical solution and Table 2 the numerical one. In comparing the results for this sample with the previous smaller sample measured in oil, several points are worth noting. First, the precision on the oil-immersed sample is significantly better, as can be seen for

**Figure 3.** The set up used to collect extinction data in air for centimeter-sized single crystals. The objective and substage systems have been removed from the microscope, and sheet polarizers were placed above and below the sample with the vibration directions crossed. Next, extinction positions are observed at the differing *S* settings (as is typical for use of EXCALIBR) by looking straight down on the sample with the naked eye.

the *R*-squared, Es-Calc(Es) columns, the ese (estimated standard error) values for 2V, and ese values for the optical orientations (Table 2). Also, the observed extinction positions and calculated extinction curves do not match as well (compare Figs. 2 and 4). However, the values of 2V are the same and the optical orientations for the sample in air have errors of 1 to 2° as compared to those of <0.5° for the sample in oil. Thus, EXCALIBRW is shown to calculate values for the orientation of the indicatrix and 2V of a sample in air that compare favorably to those in oil.

### Uniaxial vs. biaxial differentiation

To further demonstrate the utility of the graphical output of EXCALIBRW, and extinction measurements in air, an angular quartz crystal was selected to show how extinction measurements could be used to differentiate between an uniaxial and a biaxial mineral. Figure 5 is the graphical output and Table 3 lists the numerical results for the quartz crystal (note that the uniaxial model was selected for this analysis, rather than the biaxial one). Figure 6 shows the quartz sample oriented with $S$ = 20.3° and $Ms$ = 222.8°, the orientation to align E (i.e., the *c*-axis) E-W, obtained from the numerical results (Table 3). Notice how the linear upper portion of the crystal is aligned E-W with these settings. This linear feature marks the intersections of (hk0) faces. Also, compare the graphical output of the quartz measurements in Figure 5 to those of olivine (Figs. 2 and 4). Notice how the equatorial extinction curve (so called because it crosses the center line, E = 90°, of the stereographic projection) plots as a great circle. This uniaxial curve lacks the undulatory shape observed for biaxial minerals and can be used to differentiate a uniaxial

**TABLE 2.** Input data and results for large single crystal of olivine with the extinction positions measured in air; graphical results are shown in Figure 4

san carlos in air
Experimental Treatment ID number = 999.0
Refined Reference Azimuth, *Mr* = 186.61
Biaxial Results
Counterclockwise Stage
Number of iterations(100 max.) = 14
*R*-squared = 0.98972

| *S* | *M*s | *E*s | CALC(*Es*) | *Es*-CALC(*Es*) |
|---|---|---|---|---|
| 0.00 | 28.20 | 21.59 | 20.05 | 1.54 |
| 10.00 | 27.90 | 21.29 | 21.13 | 0.16 |
| 20.00 | 26.10 | 19.49 | 20.61 | −1.12 |
| 30.00 | 24.50 | 17.89 | 18.96 | −1.07 |
| 40.00 | 23.50 | 16.89 | 16.73 | 0.16 |
| 50.00 | 21.20 | 14.59 | 14.36 | 0.23 |
| 60.00 | 19.70 | 13.09 | 12.09 | 1.00 |
| 70.00 | 17.10 | 10.49 | 10.02 | 0.47 |
| 80.00 | 14.10 | 7.49 | 8.13 | −0.64 |
| 90.00 | 11.90 | 5.29 | 6.36 | −1.07 |
| 100.00 | 11.10 | 4.49 | 4.61 | −0.12 |
| 110.00 | 10.00 | 3.39 | 2.76 | 0.63 |
| 120.00 | 6.50 | 179.89 | 180.64 | −0.75 |
| 130.00 | 5.80 | 179.19 | 178.08 | 1.11 |
| 140.00 | 2.10 | 175.49 | 174.89 | 0.60 |
| 150.00 | 357.90 | 171.29 | 171.00 | 0.29 |
| 160.00 | 353.20 | 166.59 | 166.70 | −0.11 |
| 170.00 | 349.20 | 162.59 | 162.72 | −0.13 |
| 180.00 | 345.70 | 159.09 | 159.95 | −0.86 |

Optic Axial Angle, 2V (ese) = 91.454 (3.423)

Computed Cartesian Coordinates

| | x (ese) | y (ese) | z (ese) |
|---|---|---|---|
| OA1 | 0.5943 (0.0228) | 0.2284 (0.0310) | 0.7712 (0.0192) |
| OA2 | −0.7439 (0.0220) | −0.2574 (0.0324) | 0.6167 (0.0245) |
| AB | 0.9345 (0.0032) | 0.3392 (0.0086) | 0.1079 (0.0062) |
| OB | −0.1072 (0.0114) | −0.0208 (0.0446) | 0.9940 (0.0005) |
| ON | 0.3395 (0.0109) | −0.9405 (0.0035) | 0.0169 (0.0451) |

Spindle Stage Coordinates to measure refractive indices.

| | *S* (ese) | *Es* (ese) | *Ms* | |
|---|---|---|---|---|
| OA1 | 73.50 (2.30) | 53.54 (1.62) | | |
| OA2 | 112.66 (2.77) | 138.07 (1.89) | (e-w polr.) | (n-s polr.) |
| AB | 17.64 (1.03) | 20.85 (0.52) | 207.46 | 117.46 |
| OB | 91.20 (2.57) | 96.15 (0.66) | 282.76 | 192.76 |
| ON | 178.97 (2.75) | 70.16 (0.67) | 256.77 | 166.77 |

*Note:* A photo of the data collection set up and sample are shown in Figure 3.

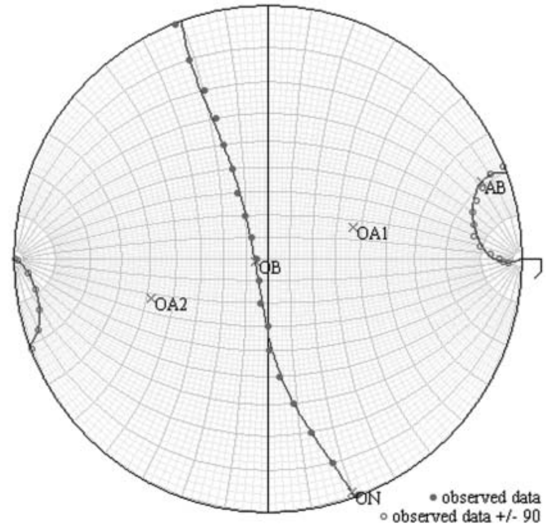


**FIGURE 4.** Graphical output for the large olivine sample shown in Figure 3 measured in air. This output corresponds to the numerical output in Table 2.

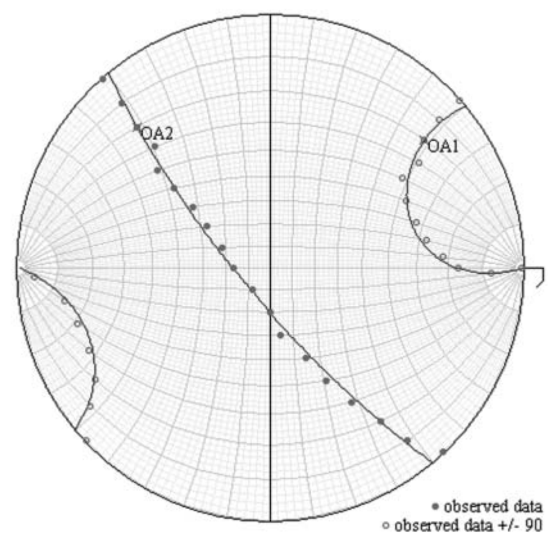


**FIGURE 5.** Graphical output for a large single crystal of quartz mounted on a goniometer head with fingernail polish. The numerical output is shown in Table 3. Note that, for the case of an uniaxial crystal, one of the extinction curves plots as a great circle whose pole is the single optic axis. Thus, one can visually differentiate between uniaxial and biaxial minerals based on the shape of the extinction curves.

crystal from biaxial one. The equatorial curve for a uniaxial crystal will plot as a great circle whose pole is the single optic axis. Also, note in the numerical and graphical output that the precision of the extinction data collected in air is similar to that of the large olivine crystal in Figure 4 and Table 2.

**Table 3.** Input data and results for a quartz crystal (shown in Fig. 6) whose extinction positions were determined in air

quartz, big crystal in air
Experimental Treatment ID number = 999.0
Refined Reference Azimuth, *Mr* = 181.34
Uniaxial Results
Counterclockwise Stage
Number of iterations(100 max.) = 9
*R*-squared = 0.98587

| *S* | *M*s | *E*s | CALC(*E*s) | *E*s-CALC(*E*s) |
|---|---|---|---|---|
| 0.00 | 43.00 | 41.66 | 39.67 | 1.99 |
| 10.00 | 43.00 | 41.66 | 41.02 | 0.63 |
| 20.00 | 43.00 | 41.66 | 41.48 | 0.17 |
| 30.00 | 40.80 | 39.46 | 41.07 | −1.62 |
| 40.00 | 43.00 | 41.66 | 39.77 | 1.88 |
| 50.00 | 39.30 | 37.96 | 37.52 | 0.43 |
| 60.00 | 33.50 | 32.16 | 34.23 | −2.07 |
| 70.00 | 29.00 | 27.66 | 29.76 | −2.11 |
| 80.00 | 22.80 | 21.46 | 24.04 | −2.58 |
| 90.00 | 18.20 | 16.86 | 17.05 | −0.20 |
| 100.00 | 9.30 | 7.96 | 8.98 | −1.03 |
| 110.00 | 1.80 | 0.46 | 0.26 | 0.19 |
| 120.00 | 356.70 | 175.36 | 171.52 | 3.83 |
| 130.00 | 347.00 | 165.66 | 163.40 | 2.26 |
| 140.00 | 340.50 | 159.16 | 156.34 | 2.82 |
| 150.00 | 333.70 | 152.36 | 150.54 | 1.81 |
| 160.00 | 327.00 | 145.66 | 146.00 | −0.35 |
| 170.00 | 323.30 | 141.96 | 142.64 | −0.68 |
| 180.00 | 318.20 | 136.86 | 140.33 | −3.48 |

Computed Cartesian Coordinates

| | x (ese) | y (ese) | z (ese) |
|---|---|---|---|
| Epsilon | 0.7492 (0.0058) | 0.6213 (0.0074) | 0.2298 (0.0115) |

Spindle Stage Coordinates to measure refractive indices.

| | *S* | *E*s | *M*s (e-w polr.) | *M*s (n-s polr.) |
|---|---|---|---|---|
| Epsilon | 20.30 | 41.48 | 222.83 | 132.83 |
| Omega | 20.30 | 131.48 | 312.83 | 222.83 |

*Note:* Graphical results are shown in Figure 5.

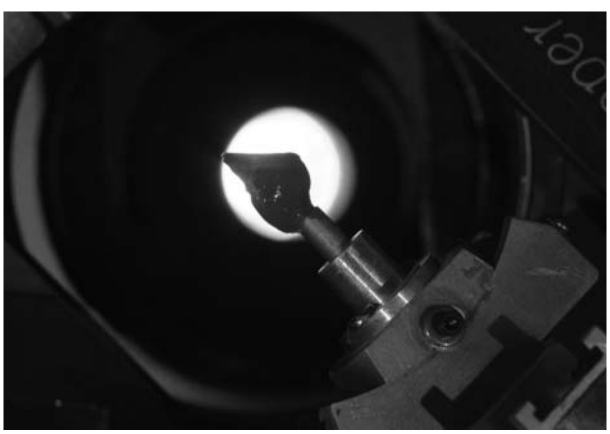

**Figure 6.** A view down the light path through the two polarizers showing the quartz crystal from Figure 5 oriented with its **c**-axis E-W based upon the *S* and *M*s values given in Table 3. This orientation can be confirmed based upon the intersection of the (*hk*0) faces (i.e., the trace of the faces parallel to **c**) being oriented E-W.

## Sample shapes

The next two examples use an angular spodumene crystal bounded by prominent cleavage faces and a sphere of olivine. Figure 7 shows the spodumene crystal mounted on the goniometer head with epoxy; Table 4 is its numerical output and Figure 8 its graphical output. The orientation of this sample also was checked on a single-crystal X-ray diffractometer and its **b**-axis found to be within 1° of the optical output. Notice, again, the

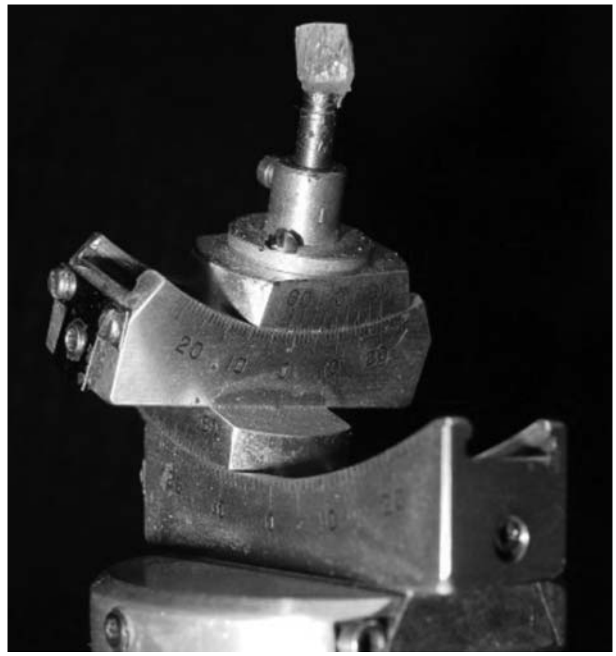

**Figure 7.** A photograph of the spodumene crystal mounted with epoxy on the end of a goniometer head. Notice the size and angular nature of this sample. EXCALIBRW results for this sample are given in Table 4 and Figure 8.

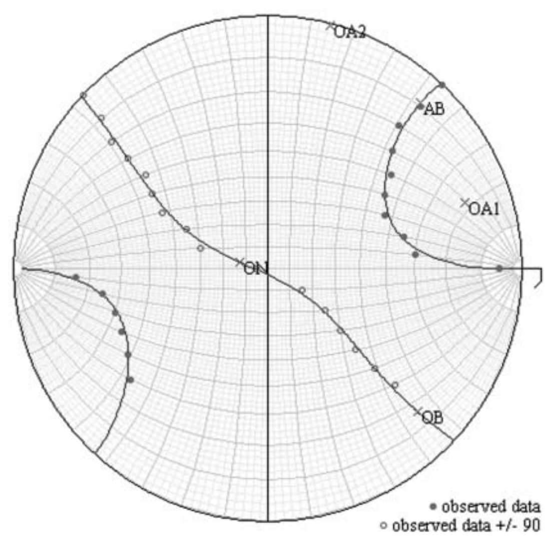


**Figure 8.** Graphical output for a large spodumene crystal (Fig. 7) whose extinction data were collected in air. Numerical results are given in Table 4.

**TABLE 4.** Input data and results for a spodumene crystal shown in Figure 7

spodumene for Raman in air
Experimental Treatment ID number = 999.0
Refined Reference Azimuth, *Mr* = 95.32
Biaxial Results
Counterclockwise Stage
Number of iterations(100 max.) = 19
*R*-squared = 0.98090

| *S* | *M*s | *E*s | CALC(*E*s) | *E*s-CALC(*E*s) |
|---|---|---|---|---|
| 0.00 | 52.00 | 136.68 | 137.15 | –0.47 |
| 10.00 | 52.50 | 137.18 | 137.84 | –0.66 |
| 20.00 | 54.60 | 139.28 | 138.02 | 1.27 |
| 30.00 | 53.10 | 137.78 | 137.61 | 0.17 |
| 40.00 | 50.00 | 134.68 | 136.53 | –1.84 |
| 50.00 | 50.10 | 134.78 | 134.54 | 0.25 |
| 60.00 | 48.20 | 132.88 | 131.19 | 1.69 |
| 70.00 | 40.00 | 124.68 | 125.45 | –0.77 |
| 80.00 | 35.00 | 119.68 | 114.88 | 4.80 |
| 90.00 | 10.50 | 95.18 | 96.51 | –1.33 |
| 100.00 | 349.50 | 74.18 | 77.54 | –3.36 |
| 110.00 | 340.60 | 65.28 | 65.94 | –0.66 |
| 120.00 | 335.00 | 59.68 | 59.03 | 0.65 |
| 130.00 | 330.90 | 55.58 | 54.30 | 1.28 |
| 140.00 | 326.10 | 50.78 | 50.74 | 0.04 |
| 150.00 | 321.90 | 46.58 | 47.94 | –1.36 |

Optic Axial Angle, 2V (ese) = 57.606 (3.036)

Computed Cartesian Coordinates

| | x (ese) | y (ese) | z (ese) |
|---|---|---|---|
| OA1 | 0.9293 (0.0112) | 0.3139 (0.0308) | 0.1945 (0.0307) |
| OA2 | 0.2482 (0.0207) | 0.9687 (0.0053) | 0.0052 (0.0280) |
| AB | 0.6719 (0.0058) | 0.7318 (0.0056) | 0.1139 (0.0122) |
| OB | 0.7069 (0.0131) | –0.6795 (0.0071) | 0.1964 (0.0553) |
| ON | –0.2212 (0.0422) | 0.0514 (0.0380) | 0.9739 (0.0114) |

Spindle Stage Coordinates to measure refractive indices.

| | *S* (ese) | *E*s (ese) | *M*s | |
|---|---|---|---|---|
| OA1 | 31.78 (5.13) | 21.67 (1.74) | | |
| OA2 | 0.31 (1.65) | 75.63 (1.23) | (e-w polr.) | (n-s polr.) |
| AB | 8.85 (0.95) | 47.79 (0.45) | 143.11 | 233.11 |
| OB | 163.88 (4.39) | 45.02 (1.06) | 140.34 | 230.34 |
| ON | 86.98 (2.26) | 102.78 (2.48) | 198.10 | 108.10 |

*Note:* Graphical results are shown in Figure 8.

**TABLE 5.** Input data and results for a sphere of olivine shown in Figure 9

olivine sphere
Experimental Treatment ID number = 999.0
Refined Reference Azimuth, *Mr* = 181.45
Biaxial Results
Counterclockwise Stage
Number of iterations(100 max.) = 13
*R*-squared = 0.98638

| *S* | *M*s | *E*s | CALC(*E*s) | *E*s-CALC(*E*s) |
|---|---|---|---|---|
| 0.00 | 38.30 | 36.85 | 36.98 | –0.12 |
| 10.00 | 38.20 | 36.75 | 37.01 | –0.25 |
| 20.00 | 41.10 | 39.65 | 39.93 | –0.28 |
| 30.00 | 50.30 | 48.85 | 48.27 | 0.58 |
| 40.00 | 65.50 | 64.05 | 65.24 | –1.18 |
| 50.00 | 85.90 | 84.45 | 82.53 | 1.93 |
| 60.00 | 92.50 | 91.05 | 92.13 | –1.08 |
| 70.00 | 98.90 | 97.45 | 97.45 | 0.00 |
| 80.00 | 102.60 | 101.15 | 101.14 | 0.02 |
| 90.00 | 106.50 | 105.05 | 104.35 | 0.71 |
| 100.00 | 109.50 | 108.05 | 107.67 | 0.39 |
| 110.00 | 112.90 | 111.45 | 111.45 | 0.00 |
| 120.00 | 115.80 | 114.35 | 115.96 | –1.61 |
| 130.00 | 123.00 | 121.55 | 121.24 | 0.32 |
| 140.00 | 129.40 | 127.95 | 127.01 | 0.94 |
| 150.00 | 133.60 | 132.15 | 132.68 | –0.53 |
| 160.00 | 139.10 | 137.65 | 137.54 | 0.11 |
| 170.00 | 142.50 | 141.05 | 141.08 | –0.03 |

Optic Axial Angle, 2V (ese) = 89.962 (0.990)

Computed Cartesian Coordinates

| | x (ese) | y (ese) | z (ese) |
|---|---|---|---|
| OA1 | 0.2384 (0.0080) | –0.6230 (0.0084) | 0.7450 (0.0071) |
| OA2 | –0.6361 (0.0077) | 0.4790 (0.0091) | 0.6049 (0.0082) |
| AB | –0.2812 (0.0069) | –0.1018 (0.0106) | 0.9542 (0.0030) |
| OB | 0.6186 (0.0050) | –0.7795 (0.0043) | 0.0991 (0.0057) |
| ON | 0.7337 (0.0057) | 0.6181 (0.0055) | 0.2821 (0.0113) |

Spindle Stage Coordinates to measure refractive indices.

| | *S* (ese) | *E*s (ese) | *M*s | |
|---|---|---|---|---|
| OA1 | 129.90 (0.64) | 76.21 (0.47) | | |
| OA2 | 51.63 (0.78) | 129.50 (0.57) | (e-w polr.) | (n-s polr.) |
| AB | 96.09 (0.65) | 106.33 (0.41) | 287.77 | 197.77 |
| OB | 172.76 (0.43) | 51.79 (0.37) | 233.23 | 143.23 |
| ON | 24.53 (0.93) | 42.80 (0.48) | 224.25 | 134.25 |

*Note:* Graphical results are shown in Figure 10.

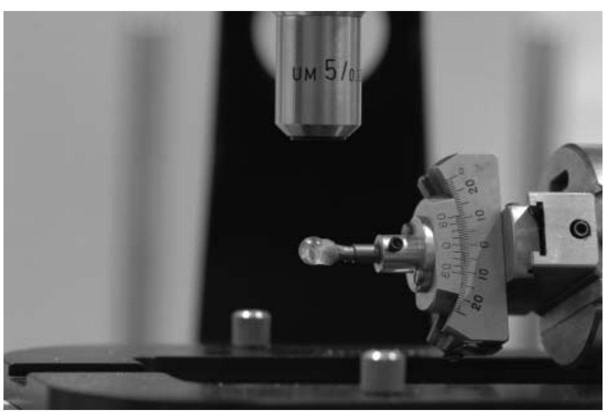

**FIGURE 9.** A close-up photograph of a 4 mm sphere of olivine mounted on the end of goniometer head with beeswax. Extinction data were collected for this sample with the objective and substage optical systems of the microscope replaced, which differs from the setup used for the other three large samples shown above. This setup was chosen because the spheres could be observed easily with a lower-power objective and it shows the method would also work with a more standard optical setup.

precision of the results are similar to quartz and the large olivine sample. Also notice that extinction values could not be obtained for $S$ = 160, 170, and 180°, yet EXCALIBRW found an acceptable solution for the data set. Lastly, an extinction data set was collected for a sphere of olivine (Fig. 9). For this sample, the Leitz Ortholux was returned to its normal configuration (i.e., substage condenser and objective systems reinstalled). As stated above, in the case of a sphere, normal incidence will occur regardless of the spindle stage setting; thus, more precise extinction data can be collected. This is shown in the increased precision in the numerical (Table 5) and graphical (Fig. 10) output. In fact, these data for the sphere are similar to those of the single crystal immersed in an index-matching fluid, with the exception of the $R$-squared values.

## ACKNOWLEDGMENTS

We thank George Rossman for providing the San Carlos olivine sample and Jim Boesenberg for providing the olivine sphere. Also, we thank Dan Kile and Tony Morse for helpful reviews; their comments improved the manuscript. Gunter also thanks the National Science Foundation (NSF-CCLI 0127191) for partial support of this project.

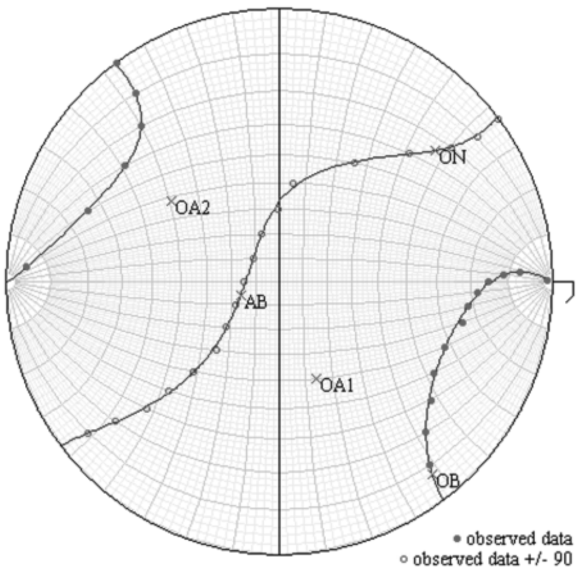


**FIGURE 10.** Graphical results for the olivine sphere shown in Figure 9; corresponding numerical results are given in Table 5.

## REFERENCES CITED


Bandli, B.R. and Gunter, M.E. (2001) Identification and characterization of mineral and asbestos particles using the spindle stage and the scanning electron microscope: The Libby, Montana, U.S.A. amphibole-asbestos as an example. The Microscope, 49, 191–199.

Bartelmehs, K.L., Bloss, F.D., Downs, R.T., and Birch, J.B. (1992) EXCALIBR II. Zeitschrift für Kristallographie, 199, 185–196.

Bloss, F.D. (1981) The Spindle Stage: Principles and Practice. Cambridge University Press, U.K.

——— (1999) Optical Crystallography. Mineralogical Society of America, Washington, D.C.

Bloss, F.D. and Riess, D. (1973) Computer determination of 2V and indicatrix orientation from extinction data. American Mineralogist, 58, 1052–1061.

Dyar, M.D., Gunter, M.E., Delaney, J.S., Lanzarotti, A., and Sutton, S.R. (2002a) Use of the spindle stage for orientation of single crystals for microXAS: Isotropy and anisotropy in Fe-XANES spectra. American Mineralogist, 87, 1500–1504.

——— (2002b) Systematics in the structure and XANES spectra of pyroxenes, amphiboles, and micas as derived from oriented single crystals. Canadian Mineralogist, 40, 1347–1365.

Gunter, M.E. (2004) The polarizing light microscope: Should we teach the use of a 19th century instrument in the 21st century? Journal of Geoscience Education, 52, 34–44.

Gunter, M.E. and Twamley, B. (2001) A new method to determine the optical orientation of biaxial minerals: A mathematical approach. Canadian Mineralogist, 39, 1701–1711.

Gunter, M.E., Weaver, R., Bandli, B.R., Bloss, F.D., Evans, S.H., and Su, S.C. (2004) Results from a McCrone spindle stage short course, a new version of EXCALIBR, and how to build a spindle stage. The Microscope, 52, 1, 23–39.

Gunter, M.E., Bloss, F.D., and Su, S.C. (1988) EXCALIBR revisited. American Mineralogist, 73, 1481–1482.

Wilcox, R.E. (1959) Use of the spindle stage for determination of principal indices of refraction of crystal fragments. American Mineralogist, 44, 1272–1293.


MANUSCRIPT RECEIVED JANUARY 3, 2005
MANUSCRIPT ACCEPTED APRIL 13, 2005
MANUSCRIPT HANDLED BY BRENT OWENS